Journal of Proteomics 199 (2019) 89–101

Contents lists available at ScienceDirect

Journal of Proteomics

journal homepage: www.elsevier.com/locate/jprot

An inter-subunit protein-peptide interface that stabilizes the specific activity and oligomerization of the AAA+ chaperone Reptin

Dominika Coufalova[a,1], Lucy Remnant[b,1], Lenka Hernychova[a], Petr Muller[a], Alan Healy[c], Srinivasaraghavan Kannan[d], Nicholas Westwood[c], Chandra S. Verma[d,e,f], Borek Vojtesek[a,2], Ted R. Hupp[a,b,g,*,2], Douglas R. Houston[h,2]

[a] Regional Centre for Applied Molecular Oncology, Masaryk Memorial Cancer Institute, 656 53 Brno, Czech Republic
[b] University of Edinburgh, Institute of Genetics and Molecular Medicine, Edinburgh, Scotland EH4 2XR, United Kingdom
[c] St Andrews University, St Andrews, Scotland, United Kingdom
[d] Bioinformatics Institute, Agency for Science, Technology and Research (A*STAR), 30 Biopolis Street, Matrix 07-01 138671, Singapore
[e] School of Biological Sciences, Nanyang Technological University, 60 Nanyang Drive, 637551, Singapore
[f] Department of Biological Sciences, National University of Singapore, 14, Science Drive 4, 117543, Singapore
[g] University of Gdansk, International Centre for Cancer Vaccine Science, ul. Wita Stwosza 63, 80-308 Gdansk, Poland
[h] University of Edinburgh, Institute of Quantitative Biology, Biochemistry and Biotechnology, Edinburgh, Scotland EH9 3BF, United Kingdom

A B S T R A C T

Reptin is a member of the AAA+ superfamily whose members can exist in equilibrium between monomeric *apo* forms and ligand bound hexamers. Inter-subunit protein-protein interfaces that stabilize Reptin in its oligomeric state are not well-defined. A self-peptide binding assay identified a protein-peptide interface mapping to an inter-subunit "rim" of the hexamer bridged by Tyrosine-340. A Y340A mutation reduced ADP-dependent oligomer formation using a gel filtration assay, suggesting that Y340 forms a dominant oligomer stabilizing side chain. The monomeric Reptin^{Y340A} mutant protein exhibited increased activity to its partner protein AGR2 in an ELISA assay, further suggesting that hexamer formation can preclude certain protein interactions. Hydrogen-deuterium exchange mass spectrometry (HDX-MS) demonstrated that the Y340A mutation attenuated deuterium suppression of Reptin in this motif in the presence of ligand. By contrast, the tyrosine motif of Reptin interacts with a shallower pocket in the hetero-oligomeric structure containing Pontin and HDX-MS revealed no obvious role of the Y340 side chain in stabilizing the Reptin-Pontin oligomer. Molecular dynamic simulations (MDS) rationalized how the Y340A mutation impacts upon a normally stabilizing inter-subunit amino acid contact. MDS also revealed how the D299N mutation can, by contrast, remove oligomer de-stabilizing contacts. These data suggest that the Reptin interactome can be regulated by a ligand dependent equilibrium between monomeric and hexameric forms through a hydrophobic inter-subunit protein-protein interaction motif bridged by Tyrosine-340.

Significance: Discovering dynamic protein-protein interactions is a fundamental aim of research in the life sciences. An emerging view of protein-protein interactions in higher eukaryotes is that they are driven by small linear polypeptide sequences; the linear motif. We report on the use of linear-peptide motif screens to discover a relatively high affinity peptide-protein interaction for the AAA+ and pro-oncogenic protein Reptin. This peptide interaction site was shown to form a 'hot-spot' protein-protein interaction site, and validated to be important for ligand-induced oligomerization of the Reptin protein. These biochemical data provide a foundation to understand how single point mutations in Reptin can impact on its oligomerization and protein-protein interaction landscape.

1. Introduction

The AAA+ superfamily contains a group of ATP-regulated hexameric proteins that are highly conserved in evolution [1]. Their dynamic oligomeric properties provide a model system to understand allosteric regulation of polypeptide assembly and function [2]. The RuvBl1/2 orthologues, also named Reptin and Pontin, represent two representative AAA+ protein members. Structural studies have defined the properties of complexes of homo-oligomeric Pontin [3], hetero-dodecameric Pontin and Reptin [4] and homo-hexameric Reptin [5]. There are two ATP-binding motifs in such AAA+ proteins: the Walker A and Walker B ATP-binding motifs that mediate ATP binding and hydrolysis respectively.

Reptin's key evolutionarily conserved activity, from yeast to vertebrates, regulates chromatin-modifying machinery, including Ino80 [6,7], and SCRAP [8]. Additional protein-protein interactions from studies in human cancer include those with ATF2 [9], Myc [10], transcription associated protein β-catenin [11], tumor suppressor ARF [12],

* Corresponding author at: Regional Centre for Applied Molecular Oncology, Masaryk Memorial Cancer Institute, 656 53 Brno, Czech Republic.
E-mail address: ted.hupp@ed.ac.uk (T.R. Hupp).
[1] Joint first authors.
[2] Joint corresponding authors.

https://doi.org/10.1016/j.jprot.2019.02.012
Received 24 October 2018; Received in revised form 16 January 2019; Accepted 23 February 2019
Available online 09 March 2019
1874-3919/

and the oncogenic protein AGR2 [13]. Reptin and Pontin are also regulators of all PIKK (phosphatidylinositol 3-kinase-related protein kinase) members [14] that in turn mediate the DNA damage response and nonsense-mediated mRNA decay (NMD). Reptin and Pontin also regulate the assembly of the telomerase holoenzyme through interactions with TERT and dyskerin [15]. A major paradigm in Reptin structure and function was identified using yeast models where it forms a multi-subunit chaperonin complex with HSP90 [16].

Reptin is a potential drug target in cancer due to its oncogenic nature and large ATP-binding pocket that might make it suitable for drug-discovery programmes [17]. As such, we had previously performed in silico screening of a large chemical library to identify several lead molecules that can interact with the Walker A ATP-binding site [18]. The screen resulted in the small molecule *Liddean* which: (i) mimicked ATP or ADP in the stimulation of the oligomerization of Reptin protein; (ii) regulated Reptin's heterologous protein-protein interactions; and (iii) stimulated Reptin assembly with Pontin in cell-based systems. Together these observations suggested that occupation of the ATP-pocket of Reptin by a small molecule ATP-mimetic like *Liddean* can stimulate its oligomerization. In this report, we focus on understanding the role of ligand binding in promoting key protein-protein contacts at the oligomerization interface of Reptin during its self-oligomerization. We identified an inter-subunit hotspot in the 'rim' of the hexamer at Tyrosine-340 that plays an important role in ligand-induced oligomerization that promotes hexamer stability and regulates Reptin's specific activity.

2. Experimental procedures

2.1. Site directed mutagenesis of Reptin at D299N and at Y340A

All chemicals were obtained from Sigma unless otherwise indicated. Human Reptin was cloned into Gateway Entry clone (Invitrogen) for subsequent use. The human Reptin sequence for cloning into a new *E. coli* expression system was amplified using the following primers: forward primer 5′-GGGACAAGTTTGTACAA AAAAGCAGGCTTCCTGGAA GTTCTGTTCCAGGGGCCC ATGGCAACCGTTACAGCCACAACC-3′ and reverse primer 5′-GGGGACCACTTTGTACAAGAAAGCTGGGTCCAGGA GGTGTCCATGGTCTCG-3′. The forward primer had a *PreScission* protease cleavage site inserted. Following amplification, the polymerase chain reaction (PCR) product was first inserted into pDONR201 and then into pDEST-15 using Gateway technology (*Invitrogen*) to generate GST-tagged Reptin. Point mutations in the above mentioned plasmids were introduced using the following primers: for the Reptin D299N mutant, forward primer 5′-GAGTGCTGTTCATCAACGAGGTCCACA TGC-3′ and reverse primer 5′-GCATGTGGACCTCGTTGATGAACAGCA CTC-3′; and for the Reptin Y340A mutant, forward 5′- GAATCCGGGG CACCAGCGCCCAGAGCCCTCACGGCA-3′ and reverse 5′- GCCGTGAGG GCTCTGGGCGCTGGTGCCCCGGATTC-3″.

2.2. Expression and purification of proteins

2.2.1. Reptin WT and mutant production

Reptin proteins were expressed as indicated previously [13]. Briefly, plasmids encoding the indicated Reptin proteins were transformed into BL21-AI (Thermo Fischer Scientific). The cells were grown in LB medium (1 L) at 37 °C up to an A_{600} of 0.5. Induction of gene expression was achieved by adding arabinose to the culture (final concentration 0.2%). The bacterial culture was grown at room temperature (21 °C) for another 3 h and then pelleted by centrifugation. The lower temperature of induction (rather than 30 °C or 37 °C) gave rise to reproducible recover of Reptin protein. Cells were lysed with 30 ml of a buffer containing 10% sucrose, 50 mM HEPES, pH 8.0, 400 mM NaCl, 0.1% Triton X-100, 1 mM DTT, 1 mM benzamidine, 0.5 mg/ml lysozyme, and protease inhibitors for 30 min on ice and then sonicated for 3 × 5 s bursts to reduce the viscosity. The clarified bacterial lysate was obtained by centrifugation for 15 min at 15,000 g. The lysate was incubated with glutathione beads (0.5 ml) (GE Healthcare) for 150 min at 4 °C with rotation in a 50 ml conical tube. The beads were thoroughly washed three times by mixing the beads with 10 bead-volumes of a high salt buffer (20 mM HEPES, pH 7.5, 1 M NaCl, 1 mM DTT, and 1 mM benzamidine) to remove non-specifically bound proteins. The beads were then washed three times with 10 bead-volumes of a low salt buffer (20 mM HEPES, pH 7.5, 0.05 M NaCl, 1 mM DTT, and 1 mM benzamidine). The beads were finally washed three times with 10 bead-volumes of PreScission buffer (GE Healthcare, Uppsala, Sweden) and then resuspended in 1 bead volume (0.5 ml) of PreScission buffer. GST-tagged PreScission protease (GE Healthcare; 5 units) was added to the slurry and incubated overnight rotating in the cold room. The beads were sedimented at 2340 g for one minute and the supernatant containing cleaved Reptin protein was recovered. The purity of Reptin was confirmed using SDS-gel electrophoresis as described previously [13]. The beads were washed with an additional column volume of PreScission buffer to collect additional, but more diluted protein. The first fraction from the elution, which is more concentrated than the second fraction, was invariably used. The Reptin protein cleaved off the column using PreScission protease (GE Healthcare) was stored at 4 °C at concentrations from 0.5 mg/ml to 1 mg/ml. The protein was stable in this condition for at least 6 months.

2.2.2. AGR2 purification

His-tagged AGR2 (from [19]) was expressed in BL21-AI and purified using Ni^{2+}-nitrilotriacetic acid-agarose (Qiagen). according to the manufacturer's instructions. In detail, the cells were grown in LB medium (0.5 L) at 37 °C up to an A_{600} of 1.0 and protein was induced by adding arabinose to the culture (0.2%). The culture was grown at 30 °C for 3 h and then pelleted by centrifugation. The pellets were lysed with 40 ml of a buffer containing 20 mM Tris–HCl, pH 8.0, 150 mM NaCl, 10 mM $MgCl_2$, 0.05% Tween 20, 10% glycerol, 20 mM imidazole, pH 8.0, and 0.5 mg/ml lysozyme for 30 min on ice. The lysate was then sonicated for 3 × 5 s bursts to reduce the viscosity. The clarified bacterial lysate was obtained by centrifugation for 15 min at 15,000 g. The lysate was incubated with Ni-agarose on rotary shaker at 4 °C for 1 h to capture the AGR2 protein. The beads were washed two times in lysis buffer and three times in lysis buffer with 40 mM imidazole, and then the AGR2 protein was eluted with lysis buffer containing 150 mM imidazole. Purity was confirmed using SDS-gel electrophoresis as described [19]. AGR2 protein eluted from the column was stored at −70 °C at concentrations from 1 to 3 mg/ml. The protein was stable in this condition for at least 2 years.

2.2.3. HSP90 purification

The coding sequence of the human HSP90AA1 gene (Hsp90α, NM_001017963.2) was cloned into a pDEST17 vector containing an N-terminal His 6 ×-tag cleavable by TEV protease. All cloned genes were expressed in BL21(DE3) RIPL cells. The cells were grown in LB medium at 37 °C up to an A_{600} of 0.5. Induction of gene expression was achieved by adding isopropyl β-D-thiogalactopyranoside to the culture (final concentration 1 mM). The bacterial culture was grown at 30 °C for another 3–4 h and then pelleted by centrifugation for 15 min at 6000 *g*. The cells were resuspended in His binding buffer II (50 mM Tris, pH 8.0, 0.2 M NaCl, 2 mM $MgCl_2$, 10% glycerol). Cell suspensions were enriched with lysozyme (1 mg/ml) and PMSF (1 mM) and then sonicated. Bacterial lysates were obtained by centrifugation for 30 min at 12,000 g. His 6 -tagged Hsp90α was purified using a HisTrap column, and the His 6 x-tag was cleaved by overnight incubation with TEV protease. The protein was subsequently exchanged into His binding buffer II and then subjected to a second immobilized metal affinity chromatograph to remove His 6 x-tag and His 6-TEV. The flow-through fractions were concentrated and further processed by gel filtration using a HiPrep 16/60 Sephacryl S-200 HR column (GE Healthcare). The purity of all isolated proteins was confirmed by SDS-PAGE/Coomassie

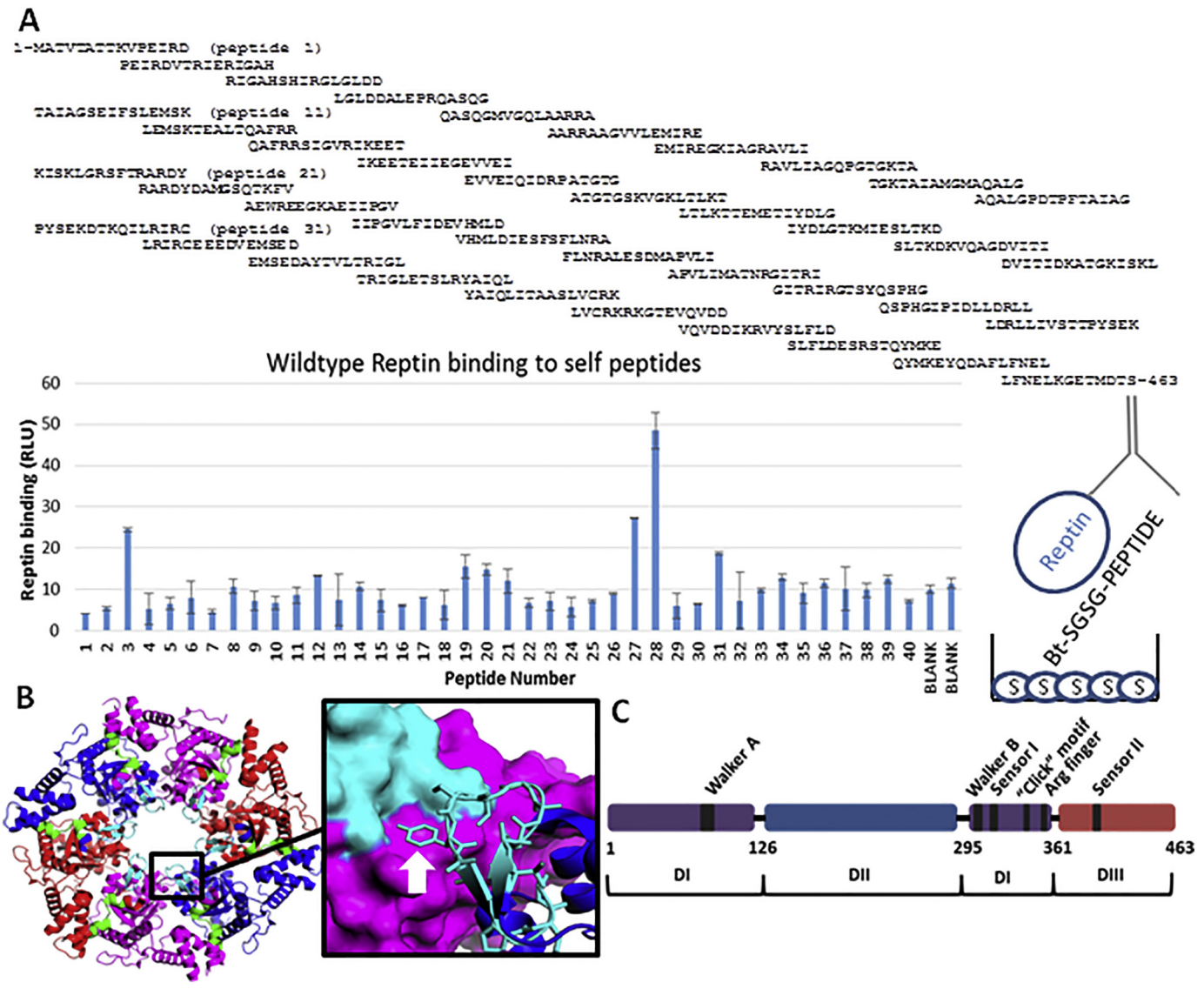

Fig. 1. Structure of Reptin (RUVBL2). (A) ELISA assay measuring the binding of wt-Reptin to self-peptides. The bottom right diagram highlights the order of addition in the Reptin binding reaction, including; (i) coating the ELISA wells with Streptavidin (S); (ii) adding the biotinylated peptide containing a SGSG space; (iii) the addition of Reptin protein; and (iv) the addition of the primary anti-reptin antibody (Y shape; in grey) that is detected using HRP conjugated secondary antibody. The top panel summarized the overlapping, biotinylated peptides derived from the Reptin open reading frame (from the N-terminus (peptide 1) through the C-terminus (peptide 40) were coated onto streptavidin ELISA wells. After washing, Reptin was added and binding measured using anti-Reptin antibody in conjunction with HRP labeled secondary antibody. Reactions were monitored via chemiluminescence. Binding data is represented by RLU (relative light units) as a function of peptide number. (B) X-ray crystal structure of the Reptin hexamer (PDB id: 3UK6) with the subunits shown in different colors (red, magenta, blue). An inter-subunit interface (428–439) is colored green and the oligomerization site (333–345) is colored aqua. (C) Details of the oligomerization site (aqua) between two Reptin monomers (blue and magenta). The side chain of the Tyrosine finger (Y340) is located in the oligomerization pocket of the second Reptin. (D). Reptin structure. A linear rod structure of Reptin domain organization. Domain DI (in purple) containing highly conserved motifs of AAA+ proteins such as the Walker A, the Walker B, the Sensor I, the Arg finger and the "Click" (inter-subunit stabilizing) motif described in this article. Domain DIII (in red) contains the conserved motif of AAA+ protein region named Sensor II. The insertion domain DIII is also highlighted. (For interpretation of the references to colour in this figure legend, the reader is referred to the web version of this article.)

staining [20]. All proteins were finally exchanged into final assay buffers using 7-kDa molecular mass cutoff Zeba spin desalting column (Thermo Fischer).

2.2.4. Reptin ELISA protein-peptide interaction assays

Overlapping biotinylated peptides were obtained from Chiron Mimotopes (Australia). Peptides derived from Reptin are displayed in the Fig. 1 legend. Reptin protein binding to biotinylated protein was measured using ELISA. Fifteen-mer peptides with a 5-mer overlap (Fig. 1A) and containing a N-terminal biotin followed by a SGSG spacer were purchased from Chiron Mimotopes. Peptides were dissolved at 5 mg/ml in DMSO. In peptide binding assays, ELISA plates were coated with streptavidin (AnaSpec) overnight at 37 °C and washed with PBS-Tween-20 (0.1% Tween-20). The biotinylated peptides diluted in water (1 μg per well) were added for 1 h followed by blocking with BSA 3% in PBS 1×. Reptin diluted in blocking buffer was then added to the plate and incubated for a further 1 h. When ligands such as ADP or *Liddean* were used, the chemicals were added to buffer containing Reptin for 30 min prior to addition of the reactions to the ELISA wells to allow sufficient oligomerization of the protein induced by the ligands. Blocking buffer and DMSO only controls were included. After further washes, wells were incubated with the Reptin primary antibody and

then horseradish peroxidase conjugated secondary antibody for 1 h each at room temperature followed by further washing and ECL addition and the luminescence produced was measured. The data are presented as Relative Light Units and represent triplicates graphed as a mean with error bars representing the deviations from the mean.

2.2.5. Gel filtration

Reptin and the indicated mutants (Y340A and D299N; 25 μg) were incubated without ligand or with ligand (1 mM ADP) in 100 μl of HEPES buffer (pH 7.6) containing PBS. Samples were injected onto a 25 ml Superose-12 gel filtration column in the same buffer and fractions were collected at a flow rate of 0.5 ml/min. In the ligand bound state, the column was pre-incubated in the same buffer but including 1 mM ADP. Gel filtration markers were used to calibrate the column and to demonstrate ADP did not alter the elution of marker proteins (data not shown). Samples eluting from the column (50 μl) of each fraction were absorbed onto ELISA wells overnight in a cold room and wells were incubated with PBS with BSA (3%) to block reactive interaction sites. The wells were washed with PBS (containing 0.1% Tween-20) (0.1%) followed by incubation with the anti-Reptin antibody (1:1000; Abcam) in PBS-tween-20 (0.1%) including BSA (3%). Reactions were processed with HRP-conjugated secondary antibodies (DAKO; 1:1000) to define the elution profile of Reptin (in RLU, chemiluminescence). The elution profiles are highlighted in Fig. 3. Molecular mass markers (GE Healthcare) that calibrated the column were injected (100 μl) at 10 mg/ml concentrations (in deionized water) and elution peak volumes were defined by absorbance ($_{max}$280 nm).

2.3. Experimental design and statistical rationale for hydrogen-deuterium exchange mass spectrometry

2.3.1. Sample preparation of Reptin proteins

Reptin, either wt or mutant (5 μM), was incubated with 1 mM ATP for 1 h at 21 °C prior to the exchange. The exchange was initiated by a sequential dilution into deuterated buffer (50 mM Tris-HCl pD 7.1, 150 mM NaCl, 1 mM EDTA, 2 mM $MgCl_2$ and 1 mM DTT) to a final concentration of 2 μM. The sequential dilution took approximately 25 s. Counting of the incubation time was initiated after addition of the first aliquot of deuterated buffer. For sample with ATP the deuterated buffer was enriched with 1 mM ATP. The exchange was carried out at room temperature and was quenched by the addition of 1 M HCl in 1 M glycine at 5 min followed by rapid freezing in liquid nitrogen.

2.3.2. Digestion and HPLC separation

Each sample was thawed and injected onto an immobilized pepsin column (15 μl bed volume, flow rate 20 μl/min, 2% acetonitrile/0.05% trifluoroacetic acid). Peptides were trapped and desalted on-line on a peptide microtrap (Michrom Bioresources, Auburn, CA) for 2 min at flow rate 20 μl/min. Next, the peptides were eluted onto an analytical column (Jupiter C18, 1.0 × 50 mm, 5 μm, 300 Å, Phenomenex, CA) and separated using a 2 min linear gradient elution of 10%–40% B buffer in A buffer, followed by 31 min isocratic elution at 40% B. Solvents used were: A buffer – 0.1% formic acid in water, B buffer – 80% acetonitrile/0.08% formic acid. The immobilized pepsin column, trap cartridge and the analytical column were kept at 1 °C.

2.3.3. Mass spectrometry and data analysis

Mass spectrometric analysis was carried out using an Orbitrap Elite mass spectrometer (Thermo Fisher Scientific) with ESI ionization on-line connected with a robotic system based on the HTS-XT platform (CTC Analytics, Zwingen, Switzerland). The instrument was operated in a data-dependent mode for peptide mapping (HPLC-MS/MS). Each MS scan was followed by MS/MS scans of the top three most intensive ions from both CID and HCD fragmentation spectra. Tandem mass spectra were searched using SequestHT against the cRap protein database (ftp://ftp.thegpm.org/fasta/cRAP) containing the sequence of the Reptin protein with the following search settings: mass tolerance for precursor ions of 10 ppm, mass tolerance for fragment ions of 0.6 Da, no enzyme specificity, two maximum missed cleavage sites and no-fixed or variable modifications were applied. The false discovery rate at peptide identification level was set to 1%. Sequence coverage was analyzed with Proteome Discoverer software version 1.4 (Thermo Fisher Scientific) and graphically visualized with MS Tools application [21]. Totally 94% of Reptin sequence was covered by 249 identified peptides (Supplementary Fig. 1). Analysis of deuterated samples was done in HPLC-MS mode with ion detection in the orbital ion trap. The MS raw files together with the list of peptides (peptide pool) identified with high confidence characterized by requested parameters (retention time, XCorr, and charge) were processed using HDExaminer version 2.2 (Sierra Analytics, Modesto, CA). The software analyzed protein and peptides behavior, created the uptake plots that showed peptide deuteration over time with calculated confidence level (high, medium confidence are accepted, low confidence is rejected). The HDX data in Figs. 5 and 7 are representative of data obtained in at least three independent experiments. The results from peptide pools (Supplementary Tables 1-3) were displayed as butterfly comparison plots (Supplementary Figs. 2-4) that showed the deuteration percentage as a function of peptide index calculated for different protein states. This function includes other useful information about how well the peptide pool covers protein (number of peptides, percentage of coverage protein sequence, standard deviation, average redundancy etc., Supplementary Figs. S2-S4). Other graphs showing the evolution of deuteration at individual parts of the protein at the same time and different protein states were plotted using the GraphPad Prism version 5.03 for Windows (GraphPad Software, San Diego, CA, USA). The bimodal isotopic envelopes were analyzed by HX-Express 2 [22]. Molecular structures were rendered using PyMOL [23]. The mass spectrometry proteomics data have been deposited to the ProteomeXchange Consortium via the PRIDE repository with the dataset identifier “PXD008226”; Username: reviewer05996@ebi.ac.uk, Password: I7pjGxG1.

2.4. Modeling and molecular dynamics (MD) simulations

MD simulations of *apo* and ADP bound monomeric and hexameric Reptin in its wt, Y340A and D299N mutant forms were carried out with the *pemed.CUDA* module of the program Amber14 [24]. The structures of the mutants (Y340A, D299N) were generated by substituting Tyr340 with Ala and Asp299 with Asn in the wild-type protein [5]. All atom versions of the Amber 14SB force field (ff14SB) [25] and the generalized Amber force field (GAFF) [26] were used to represent the protein and ADP respectively. The *Xleap* module was used to prepare the system for the MD simulations. Each structure was solvated in an octahedral box with TIP3P [27] water molecules, leaving at least 10 Å between the solute atoms and the borders of the box. All the simulation systems were neutralized with appropriate numbers of counterions. MD simulations were carried out in explicit solvent at 300 K. During the simulations, the long-range electrostatic interactions were treated with the particle mesh Ewald [28] method using a real space cutoff distance of 9 Å. The Settle [29] algorithm was used to constrain bond vibrations involving hydrogen atoms, which allowed a time step of 2 fseconds during the simulations. Solvent molecules and counterions were initially relaxed using energy minimization with restraints on the protein and inhibitor atoms. This was followed by unrestrained energy minimization to remove any steric clashes. Subsequently the system was gradually heated from 0 to 300 K using MD simulations with positional restraints (force constant: 50 kcal mol^{-1} $Å^{-2}$) on protein and inhibitors over a period of 0.25 nseconds allowing water molecules and ions to move freely. During an additional 0.25 nseconds, the positional restraints were gradually reduced followed by a 2 nseconds unrestrained MD simulation to equilibrate all the atoms. For each system, three independent MD simulations (assigning different initial velocities) were carried out for 250 nseconds with conformations saved every 10

pseconds. Figures were drawn using PyMOL [23].

3. Results

3.1. Defining hotspot Reptin interaction sites using an overlapping biotinylated Reptin self-peptide library array

Reptin forms multiple inter-subunit protein-protein interaction contacts. However, the dominating, functional interaction sites or "hotspots" that stabilize inter-subunit protein-protein interactions [30] involved in Reptin homo-oligomer assembly are not well-defined. The emerging view of protein interactions in higher eukaryotes highlights the concept that the large portion of protein-protein interactions are driven by linear peptide motifs that encompass hotspots for stabilizing domain-domain interactions [31]. We used this concept as an approach to determine whether Reptin exhibits self-binding activity towards linear peptide motifs derived from the Reptin amino acid sequence. We set up an overlapping biotinylated peptide scan assay using sequences derived from Reptin (Fig. 1A) to identify self-peptides that might interact stably with the protein. Identification of such linear peptides could point out high affinity, functional, "hotspots" in inter-subunit protein-protein docking site.

Synthetic biotinylated peptides contained a SGSG amino acid spacer followed by the appropriate overlapping Reptin amino acid sequence are listed in Fig. 1A. The biotinylated peptides were captured on streptavidin coated ELISA wells and unbound peptides was washed away. Monomeric Reptin was added to measure binding activity. There was only one major, dominating self-peptide binding activity that was mapped to peptide 28 (Fig. 1A; Biotin-SGSG-GITRIRGTSYQSPHG) which resides at an inter-subunit region of the Reptin oligomer (Fig. 1B). This peptide forms a tyrosine finger which embeds into each adjacent subunit in the hexameric structure (Fig. 1C). We name this tyrosine-containing peptide a click motif. Interestingly, deuterium exchange mass spectrometry was used previously to demonstrate that the Reptin ligand and ADP-mimetic named *Liddean* suppressed deuteration at this site within the ring structure formed between all six subunits [18]. These data are consistent with a model that oligomerization induced by *Liddean* might suppress deuteration at this buried inter-subunit interface motif.

3.2. Ligands that induce Reptin oligomerization suppress its interaction with the click interface peptide 28

We next set up assays that measure the impact of a ligand that can induce Reptin oligomerization on its binding to peptide 28. A titration of Reptin protein (up to 320 ng) into ELISA wells coated with either peptide 27, peptide 28, or peptide 29 (Fig. 1A) confirmed that the protein exhibits a high preference for peptide 28 (Fig. 2A). This peptide contains the amino acid sequence with the bridging Tyrosine 340 amino acid side chain (Fig. 1C). Using this assay, we next determined whether Reptin binding to peptide 28 can be affected by ligands that induce its oligomerization. Using fixed amount of Reptin (500 ng), increasing concentrations of ADP from 1 μM to 200 μM resulted in a reduction in its binding to peptide 28 (Fig. 2B). Similarly, increasing the concentrations of *Liddean* from 1 μM to 200 μM resulted in suppression of Reptin binding to peptide 28 (Fig. 2B). As a control, the weak binding activity of Reptin observed to peptide 27 was also reduced by increasing the concentrations of either ADP or *Liddean* (Fig. 2B). These data are consistent with the hypothesis that Reptin homo-oligomer formation stabilized through the inter-subunit docking of the peptide 28 click motif to the adjacent subunit (as in Fig. 1B and C) would sterically preclude the self-peptide 28 binding *in trans*.

We next also evaluated previously identified Reptin interacting proteins, as controls, to determine how ligand-induced oligomerization impacts on Reptin binding activity. *Liddean* was used as an ATP mimetic ligand that binds to the Walker-A ATP binding domain [18]. ADP was also used to eliminate the contribution of ATPase activity of Reptin from the Walker B ATP-interaction site to its dynamic oligomerization. AGR2 is a previously published Reptin binding protein whose binding to Reptin has been fine-mapped [18]. As expected, we observed that both *Liddean* and ADP reduced Reptin binding to AGR2 (Fig. 2C).

Reptin is part of the R2TP complex and can interact with certain molecular chaperones, including HSP90 [32]. A titration of Reptin alone resulted in relatively low levels of binding to the HSP90 chaperone (Fig. 2C). The pre-incubation of Reptin with either *Liddean* or ADP (500 μM) increased the binding activity of Reptin (Fig. 2D). *Liddean* was more potent than ADP in stimulating the HSP90-Reptin complex (Fig. 2D). This is consistent with the increased potency of *Liddean* to induce SDS-stable oligomerization of Reptin [18]. These data suggest that the ligand bound form of Reptin (presumably oligomeric) or the ligand-free form of Reptin (presumably monomeric) have different affinities for partner proteins (summarized in Fig. 4).

3.3. Mutation of tyrosine-340 within the click peptide motif reduces ligand-stimulated oligomerization of Reptin

These data can be used to predict that if we mutate the Y340-peptide oligomerization interface (Fig. 1C) we might alter Reptin oligomerization. In addition, we might also impact on the affinity of Reptin for these proteins whose binding is regulated by Reptin oligomerization states (as in Fig. 2). In order to determine whether the Y340A mutation can impact on Reptin oligomerization states, we evaluated the relative mass of the wild-type and mutant Reptin by quantifying their elution profiles using gel filtration.

Two mutant forms of Reptin were purified and characterized compared to the wild-type protein. We chose to mutate Tyrosine 340 to Alanine ($Reptin^{Y340A}$), since the Tyrosine side-chain forms a possible key hydrophobic stabilizing interaction between monomers (Fig. 1C). We then asked how the loss of this apparently stabilizing tyrosine amino acid contact (Fig. 1C) can impact on ligand-dependent oligomerization. We also chose to mutate Aspartate 299 to Asparagine ($Reptin^{D299N}$). This mutation resides within the Walker B ATP binding domain and is implicated as a gain-of-function inhibitor of Reptin in cell growth since it has enhanced ATP-binding activity [13] because of a defective ATPase activity [33]. However, to our knowledge, despite significant functional cell based data on the biochemical characteristics of this D299N mutant, there has been no analysis of its oligomerization status in the absence and presence of ligand. As such, we included this mutant as another control to evaluate how the oligomerization of Reptin might be affected in comparison to the Y340A mutation.

An ELISA assay was used to measure the elution of Reptin from a Superose-12 gel filtration column and then to define its relative oligomerization state in the ligand-free and ligand bound forms. Following elution from the gel filtration column, aliquots of the fractions were absorbed onto 250 μl ELISA wells. Protein was detected using immunochemical detection as indicated in the Experimental Procedures. We would predict at the outset that wild-type Reptin would exhibit an increase in its oligomerization status in the presence of ligand. We would predict that the $Reptin^{Y340A}$ mutant would presumably be less oligomeric if our hypothesis is accurate that the Y340 side chain forms a stabilizing hotspot interaction with the adjacent subunit. We did not know at the outset how the $Reptin^{D299N}$ mutant would elute in the absence and presence of ligand.

We processed the samples without ADP or with ADP in the gel filtration buffer (1 mM), rather than ATP, as the use of ADP removes the contribution of ATP hydrolysis to the dynamic oligomerization state of the protein over the course of the gel filtration elution (90 min). Relative to molecular mass markers, wt-Reptin elutes as an apparent monomer on S12-sepharose (Fig. 3A). The preincubation of Reptin with ADP, and including ADP in the gel filtration buffer, results in an increase in a pool of the protein at a larger mass range suggesting the elution of a stable oligomer (a hexamer based on crystal structure data).

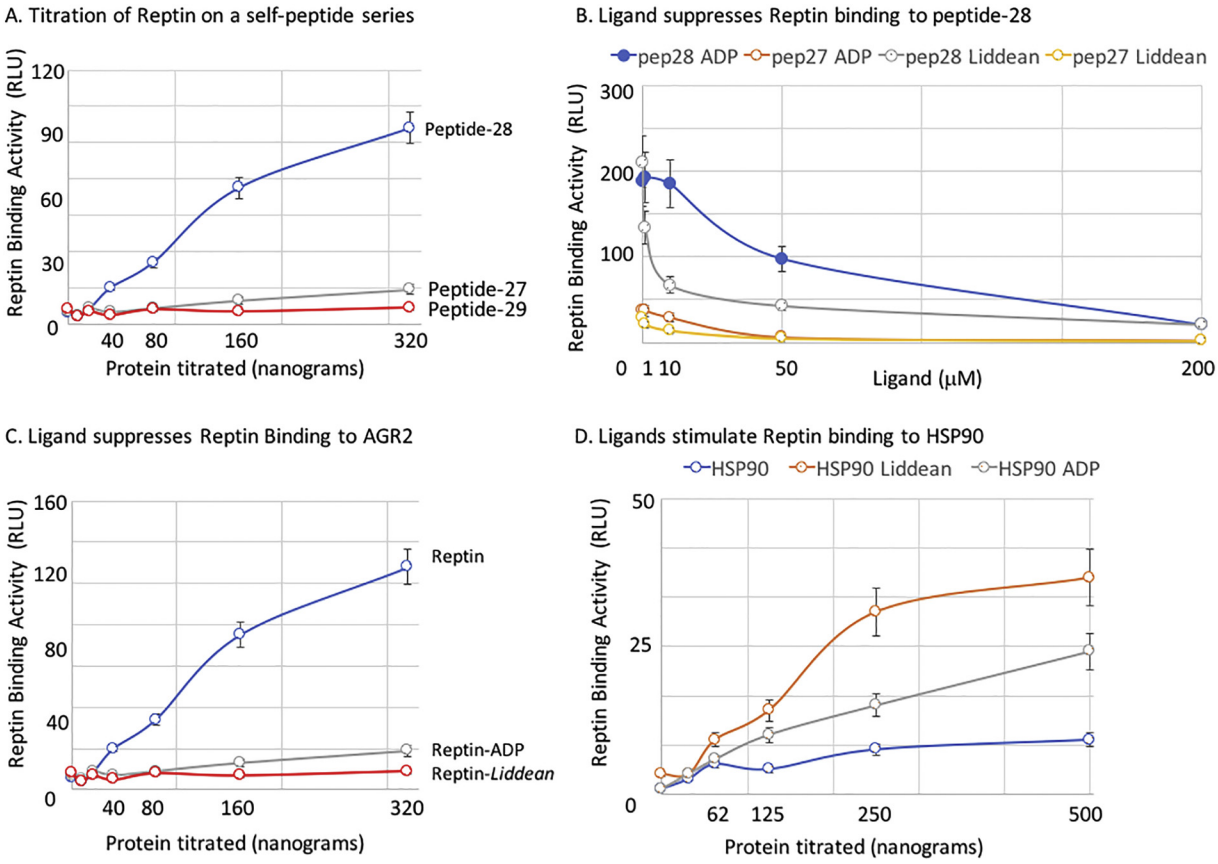

Fig. 2. Impact of ligands on the protein-binding function of Reptin. (A). ELISA wells pre-coated with streptavidin were incubated with the indicated peptides (27, 28, and 29) representing the motif surrounding the self-binding peptide (28; Fig. 1). Reptin was titrated to measure relative binding. Anti-Reptin and HRP-conjugated secondary antibodies were used to measure the extent of Reptin binding (in RLU, chemiluminescence). (B). ELISA wells pre-coated with streptavidin were incubated with the indicated peptides (27 and 28). Reptin (500 ng) was preincubated with or without increasing concentrations of the indicated ligand (DMSO), *Liddean*, or ADP) in buffer (50 μl). Anti-Reptin and HRP-conjugated secondary antibodies were used to measure the extent of Reptin binding (in RLU, chemiluminescence). (C). The previously published Reptin binding proteins (AGR2) was coated onto ELISA wells. Reptin was titrated with or without the indicated ligand (DMSO, ADP (100 μM), or *Liddean* (100 μM)). Anti-Reptin and HRP-conjugated secondary antibodies were used to measure the extent of Reptin binding (in RLU, chemiluminescence). (D). The previously identified Reptin interacting protein, HSP90, was coated onto ELISA wells. Reptin was titrated with or without the indicated ligand (DMSO, ADP (500 μM), or *Liddean* (500 μM)). Anti-Reptin and HRP-conjugated secondary antibodies were used to measure the extent of Reptin binding (in RLU, chemiluminescence).

We found that a reproducible proportion of the Reptin did not shift into the fully oligomeric (presumably hexameric) position, as highlighted by the presence of two peaks in the gel filtration elution profile (Fig. 3A). These data suggest there might be two distinct conformational pools of the recombinant Reptin purified from bacterial host (as suggested by bimodal hydrogen deuterium exchange data, see below). Alternatively, the gel filtration methodologies might dilute Reptin during the chromatography, reducing its concentration sufficiently below its association constant in the presence of ligand.

Elution of Reptin^{Y340A} protein resulted in a protein that mimicked wild-type Reptin profile in the absence of ligand but the inclusion of ADP in the buffer did not result in a shift it into a larger oligomeric state (Fig. 3B). These data suggest that the Y340 does provide a hotspot stabilization interaction between the subunits as its mutation precludes stable oligomer formation in the presence of the ligand. This is consistent with the ability of peptide-28 (containing the tyrosine 340 residue) to bind with a relatively high affinity to Reptin (Fig. 1A). As the unknown control, to our surprise, the ATP-binding gain-of-function mutant Reptin^{D299N} resulted in a profile (in the absence of ligand) that mimics wt-Reptin bound to ADP (Fig. 3C). These latter data suggest that the D299N mutant traps Reptin in an oligomeric state without ligand. These data are rationalized using molecular dynamic simulations (below) and we include this D299N mutant in our discussion on oligomer fluctuation as a comparison to the Y340A and wt forms of Reptin (Fig. 4). The data also suggest, although the D299N mutation has been defined as 'inactive' in cells due to its low ATPase activity, with respect to oligomerization, the D299N mutation induces a 'gain-of-function' property to the protein. However, since the protein is ATP hydrolysis inactive, it would presumably be not only gain-of-function with respect to oligomerization but dominant negative in its activity in cells.

Having established that the panel of wild-type and mutant proteins exhibit different oligomerization properties in the presence or absence of ligand, we next tested all in a range of biochemical assays to correlate oligomerization potential to its specific activity. This panel of Reptin proteins (wt-Reptin, Reptin^{Y340A}, Reptin^{S342A}, and Reptin^{D299N}) was next tested for binding to one of its most well-characterized binding proteins; the oncogenic AGR2 protein [13]. The binding of either wild-type Reptin or Reptin^{S342A} to AGR2 are relatively similar (Fig. 3D) suggesting that the Serine 342 site chain does not form a hot spot stabilizing interaction. Interestingly, Reptin^{D299N} exhibited a much lower specific activity in this AGR2 binding assay (Fig. 3D). Since Reptin^{D299N} exhibits enhanced oligomerization without ligand (Fig. 3C), these data are consistent with the prior data showing that that the ligand-bound form of Reptin has reduced AGR2 binding activity (Fig. 2D). By contrast, the Reptin^{Y340A} exhibited a much higher specific activity that wild-type Reptin in this AGR2 binding assay (Fig. 3D). These data are also consistent with the concept that Reptin can exist in dynamic oligomeric states. The monomeric state of the Y340A mutant (as suggested

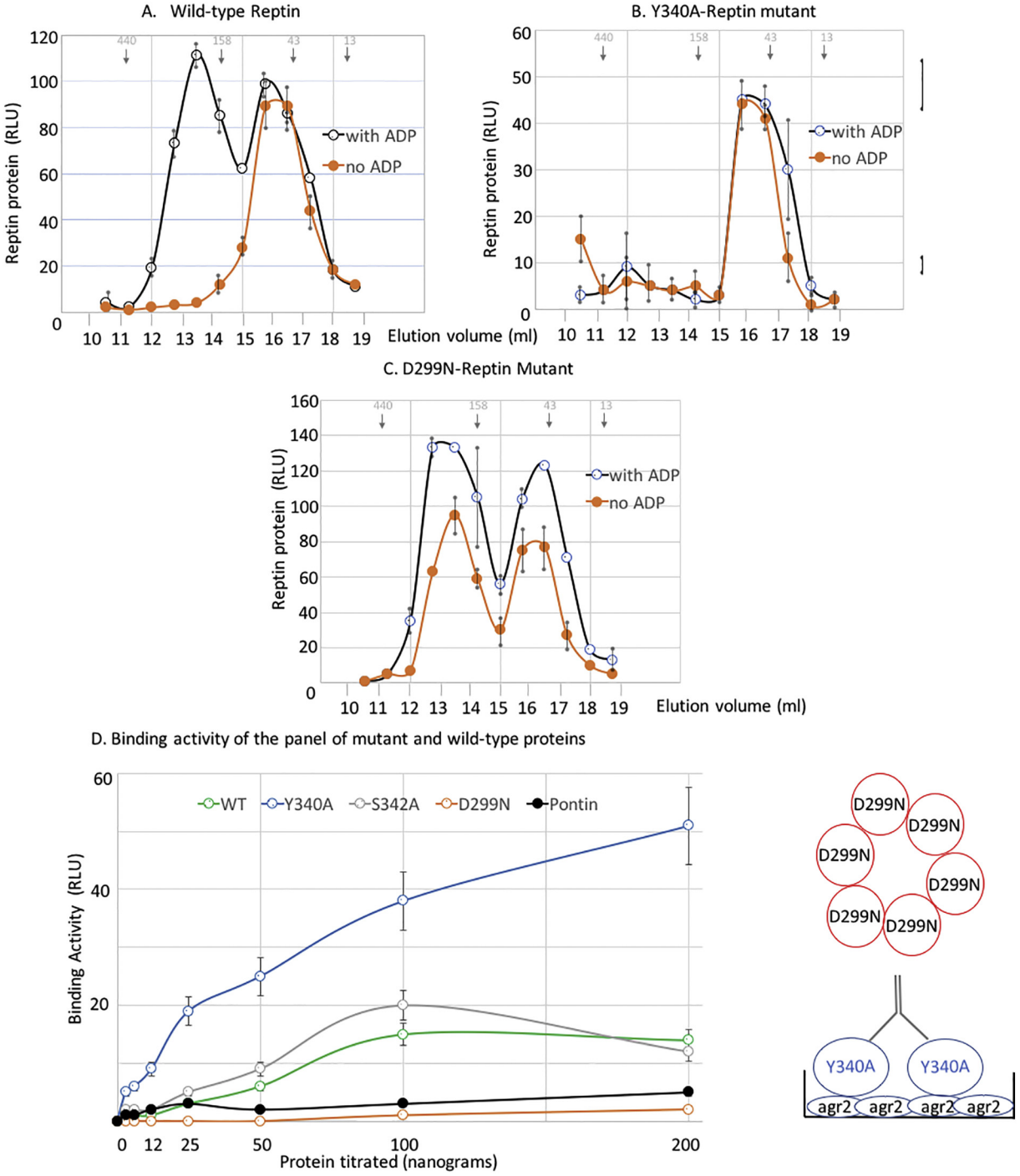

Fig. 3. The impact of mutation on Reptin quaternary structure and specific activity. (A). Wild-type Reptin, Reptin^{Y340A}, and Reptin^{D299N} were incubated with 1 mM ADP or without ligand and loaded onto a superose-12 gel filtration column (25 ml). Fractions of samples eluting from the column were absorbed onto ELISA wells. Anti-Reptin and HRP-conjugated secondary antibodies were used to measure the extent of Reptin elution and binding (in RLU, chemiluminescence). The arrows highlight the elution of molecular mass markers in kDa (440, Ferritin; 158, Aldolase; 43, Ovalbumin; 13, RNase A) in parallel processed in the absence of ADP. (B). Wild-type Reptin and the indicated mutants were analyzed in AGR2 protein binding assays. AGR2 (1 μg) was pre-coated onto ELISA wells. Reptin was titrated, and anti-Reptin and HRP-conjugated secondary antibodies were used to measure the extent of Reptin binding (in RLU, chemiluminescence). The diagram on the right interprets the data in the ELISA; mutations that drive Reptin into the monomeric state (Y340A) have a higher specific activity for AGR2, whilst mutations that stabilize Reptin in its oligomeric state (D299N) have a lower specific activity for AGR2 protein. These data are consistent with the attenuation of wild-type Reptin binding to AGR2 protein in the presence of oligomerization-promoting ligands, *Liddean* or ADP (Fig. 2).

by Fig. 3B) can increase its binding to some proteins such as AGR2 (Fig. 3D and Fig. 4).

3.4. Use of Hydrogen-deuterium exchange mass spectrometry (HDX-MS) to measure Reptin oligomerization dynamics

HDX-MS was used to measure the effect of ATP on the conformation of Reptin and the impact of the Y340A mutation on these properties.

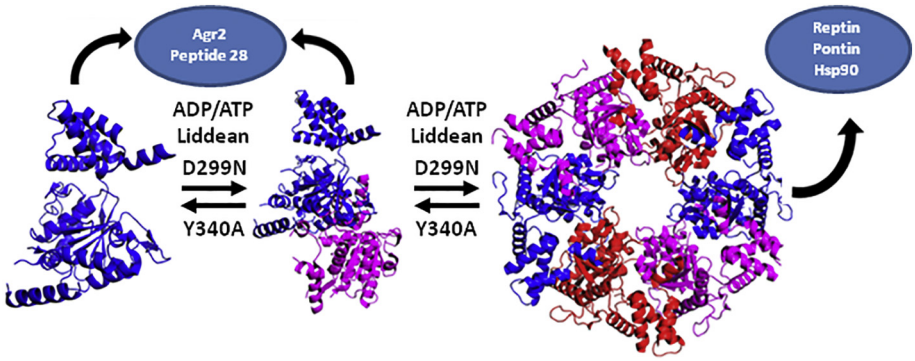

Fig. 4. A model describing the specific activity of Reptin as a function of its oligomeric state. Reptin is presented as existing in distinct dynamic oligomeric states. Mutations or ligands can impact on this flux. The reason for developing a staged model is, firstly; there is one stable inter-subunit protein-protein interface that can be detected as suppressed by HDX-MS in Reptin in the presence of ATP (Supplementary Fig. 5C and Fig. 6A). The wild-type Reptin and Y340A mutant form of Reptin exhibit similar suppression of deuteration at this inter-subunit protein-protein (Fig. 6A and B). These data suggest that the Y340A mutation has little impact on oligomer assembly at this site. By contrast, the Y340A mutation can attenuate full oligomerization at the 'rim' (Fig. 3B and Fig. 6B). By contrast to the Y340A mutation that attenuates oligomer formation, the D299N mutation stabilizes the hexameric state in the absence of ligand (Fig. 3C). The stabilization effect of the D299N mutation is rationalized in Figs. 7-9. In contrast to mutations, oligomerization (hexamerization) can be stimulated by ligands such as ATP, ADP, or *Liddean*. Oligomerization stimulation of Reptin can increase or decrease its binding to client proteins (Fig. 2). This is similar to a study on the assembly of Reptin and Pontin by Histone-3; where proteins that bind to the Reptin-Pontin system depend on the monomer to oligomer status of the two proteins [43].

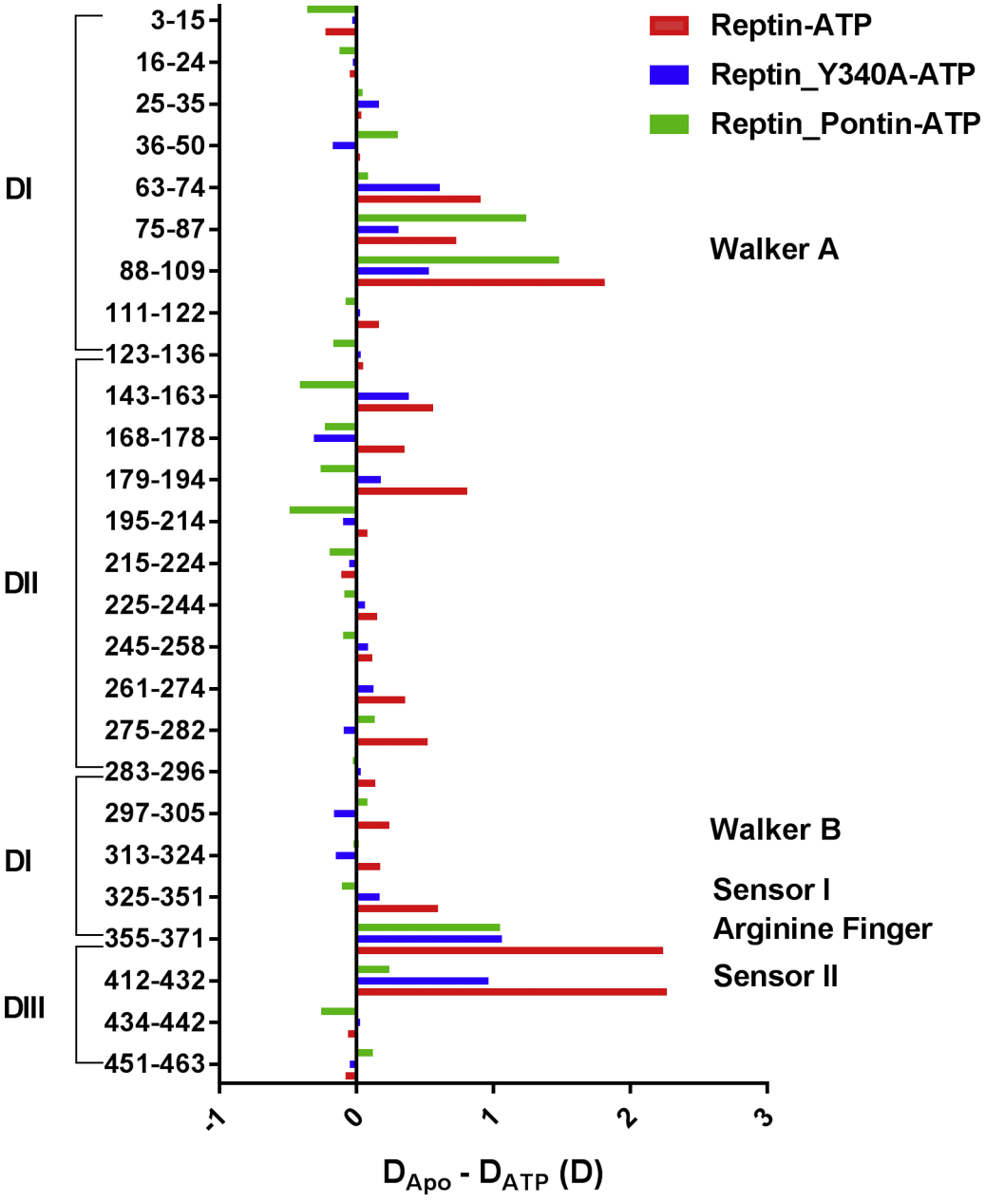

Fig. 5. Hydrogen-Deuterium exchange mass spectrometry of Reptin in differing conformational states. (A) wild-type Reptin; (B) Y340A mutant form of Reptin; (C) wild-type Reptin with Pontin. Reptin in all three conformational states (apo) was preincubated with or without ligand (ATP) and subjected to deuteration and pepsinization. The reaction products were subjected to mass spectrometry as indicated in the Experimental Procedures. The graphs highlight the change in the number of deuterons as a function of ligand from each isoform (See Supplementary Table 4). In addition, the average deuteration (%) of peptic peptides, as a function of primary amino acid sequence, of ligand-bound and ligand-free Reptin at the 300 s time point calculated as described [37] is summarized in Supplementary Fig. 6.

We have previously used HDX-MS methodology to define conformational changes induced upon mutation or ligand binding in proteins including MDM2 [34], CHIP [35], EpCAM [36], and HSP70 [37]. We first compared deuteration of wild-type Reptin with deuteration of wild-type Reptin pre-incubated with 1 mM ATP (Fig. 5 and Fig. 6A). Peptic peptide segments that exhibited different deuterium exchange rates at 300 s post-dilution with deuterated buffer as result of ATP binding are highlighted in Fig. 5 (in red). The data reflect changes in deuteron number as a function of the indicated peptic peptide fragments. These peptides are located in all three Reptin functional domains (Fig. 6A). In domain I (Fig. 1D and Fig. 6A), these segments contain amino acids 63–109 that comprise the ATP-binding Walker A motif (Supplementary Fig. 5; in white). This is consistent with ATP occupying the nucleotide binding pocket of Reptin under these conditions and serves as a positive control that the ATP-binding reaction was active under the deuteration dilution conditions. In addition, domain I containing amino acids 298–318, comprising the Walker B motif, also exhibited attenuated deuteration (Supplementary Fig. 5; in blue). This is also consistent with ligand interaction at this site leading to suppression of deuteration. A third motif in domain I includes amino acids 340–351 (Fig. 6A, in red) that contains the Tyrosine-340 residue and comprises the so-called “click” motif that is proposed to be an important stabilizing amino acid involved in inter-subunit stability (Fig. 1C). These latter data are consistent with the model that ligand binding results in hexamer formation and that this leads to lowered solvent accessibility and/or structural fluctuations of the “click” motif containing Tyrosine-340.

In domain II, also known as the insertion domain, deuterium suppression induced by ATP includes segments containing amino acids 179–194 and 275–282 (Fig. 6A; and (Supplementary Fig. 5B; in white). This domain is proposed to bind DNA and/or RNA. In domain III, which is also part of the ATP pocket, we were unable to map peptides to almost half of the domain using pepsin digestion (see grey regions in Fig. 6A). However, in the remaining part of domain III, deuteration suppression was observed in segments comprising amino acids 355–371 and 412–433 (Fig. 6A and (Supplementary Fig. 5B; in blue)). Other previously dissected functional domains of Reptin were also examined. The Arg finger (R353) was not covered by peptic peptides. The sensor I region (amino acids M326 - N329) exhibited no changes in deuteration and the sensor II region (amino acids T397 - A402) was also not covered by peptic peptides. An inter-subunit protein-protein interface (amino acids 428–439) were suppressed by ligand (Supplementary Fig. 5C; in white).

Next, we compared the deuteration of Reptin^{Y340A} and Reptin^{Y340A} with 1 mM ATP to determine the effects of reduced oligomerization (Fig. 3B) using deuteration as an assay (Fig. 5 and Fig. 6B). The presence of ATP induced structural changes in Reptin^{Y340A} which are similar to that observed with wild-type Reptin (Figs. 4 and 6; A vs B). Peptic segments that exhibited slower deuterium exchange as a result of ATP binding are highlighted in Fig. 6B (in red). In contrast to wild-type Reptin, there are two segments located in domain I and domain II (amino acids 114–123 and amino acids 275–282 respectively; highlighted in Fig. 6B, in blue colour) that exhibited increase in deuteration after incubation with ATP. These data suggest that this region in Reptin^{Y340A} becomes more exposed to solvent after ATP binding and is suggestive of a lower rate of hexamer formation. Decreases in deuteration were detected similarly as in wild-type Reptin in domain I (segments 51–74 and 90–109) and domain III (segments 355–399 and 411–433).

Interestingly no changes of deuteration were detected in the Y340 peptide docking motif (Y340) in the Reptin^{Y340A} mutant but decreases in deuteration was observed after the amino acid at position 355 (Fig. 5B and Fig. 6B). The neutral effects of ligand on the deuteration of the Y340 peptide docking motif in Reptin^{Y340A} protein are consistent with the model that loss of Tyrosine 340 precludes full “hexamerization” of the Reptin monomer.

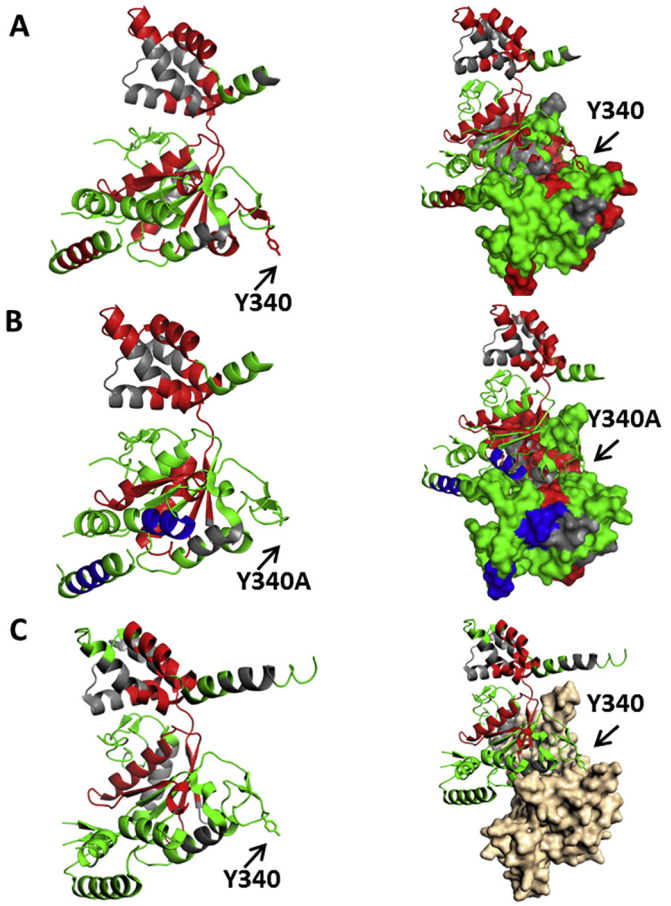

Fig. 6. Localization of deuteration flux superimposed on the three-dimensional structure of Reptin. *(A and B; wild-type Reptin and the Y340A mutant form of Reptin, respectively)*. The crystal structures of the Reptin containing one or two subunits were extracted from the hexamer crystallized as PDB code 3UK6 and the image contains regions highlighted by colors according to changes in deuteration. Red regions indicate areas of decreased deuterium exchange larger than 5% in the presence of ATP and blue regions indicate areas of increased exchange larger than 5%, whilst green indicates no significant change and grey indicates regions with no peptic peptides detected by HDX-MS. (A) The Tyrosine finger (Y340) is indicated by an arrow. (B) The Tyrosine finger (Y340) mutated to alanine is indicted by an arrow. (C). Crystal structures of the monomeric Reptin and the Reptin-Pontin complex (PDB code 2XSZ) with regions highlighted by colors according to changes in deuteration. Red regions indicate areas of decreased exchange larger than 5% in the presence of ATP, while green indicates no significant change and grey indicates regions with no peptides detected by HDX-MS. The Tyrosine finger (Y340) is indicated by arrow. The Pontin is colored light pink. The image was created in PyMOL [23]. (For interpretation of the references to colour in this figure legend, the reader is referred to the web version of this article.)

Finally, as a control, we compared the deuteration of the Reptin-Pontin complex and Reptin-Pontin complex with 1 mM ATP (Fig. 5 and Fig. 6C). Deuterium incorporation was reduced by ATP in two segments of Reptin (Fig. 5). Peptides protected by ATP in the HDX-MS analysis are highlighted on the structure of Reptin (Fig. 5). The first protected segment with reduced deuteration includes amino acids 63–109 and comprise the Walker A motif. This result is similar to that for wt Reptin and is in accordance with ATP binding to the ATP pocket. The second segment which showed reduced deuterium uptake (amino acids 355–433) belongs to domain III. As seen for Reptin^{Y340A}, the decrease of deuteration caused by ATP was observed in the region following the Y340 peptide docking motif. This suggests that the Y340 peptide docking motif does not participate in the formation of the Reptin-Pontin complex. By contrast, the Reptin-Pontin complex incubated with ligand,

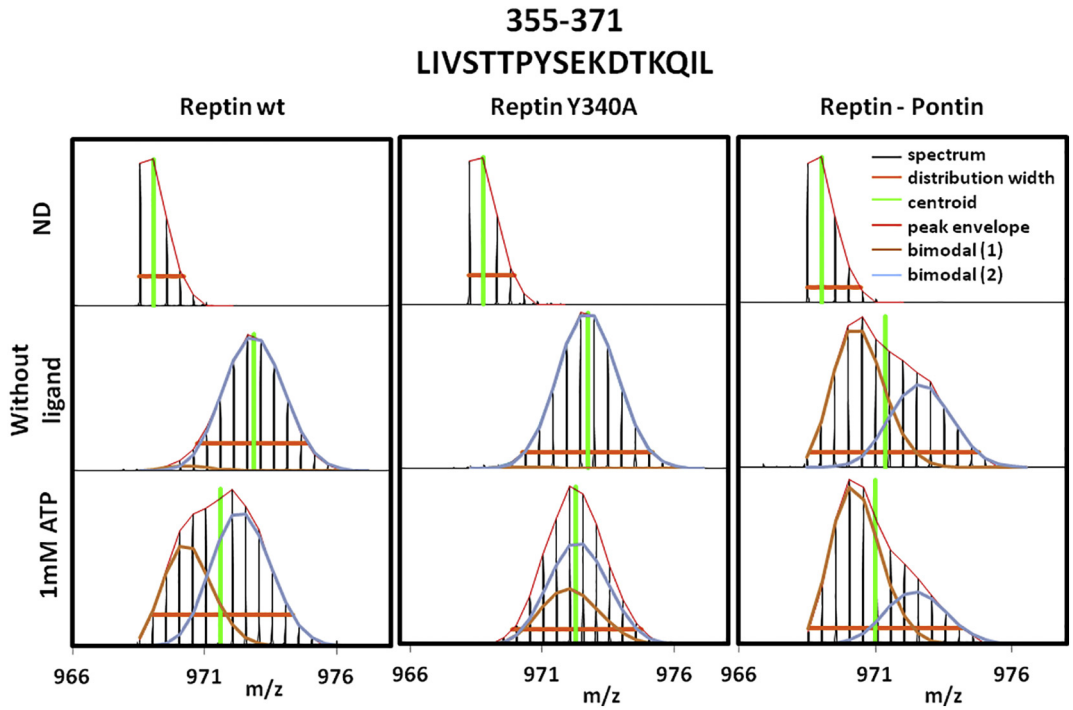

Fig. 7. Bimodal isotopic envelopes. Bimodal isotopic patterns were detected in several peptides. Shown are mass spectra of the peptide containing AAs 355–371. Spectra are shown for all three samples (Reptin wt, Reptin Y340A, and Reptin-Pontin) and for these conditions: undeuterated, sample without ligand and sample with 1 mM ATP. Clear bimodal patterns were detected in Reptin wt after incubation with ATP and in Reptin-Pontin regardless of ATP. On the other hand, Reptin Y340A did not show clear bimodal distributions in any peptides. This is consistent with the data showing that mutation of tyrosine 340 alters Reptin oligomerization. All these findings support our interpretation that bimodal patterns are caused by presence of monomeric/oligomeric state of Reptin rather than EX1 kinetics.

no changes of deuteration were detected in domain II (Fig. 5).

3.5. Bimodal distribution in MS spectra

A summary of Reptin oligomer dynamics is reviewed in Fig. 4. The oligomer dynamics in the presence of ligand can also change as a function of the absolute concentration of Reptin. The concentration of Reptin decreases upon dilution with D_2O. We might predict, therefore, that the HDX methodology can give rise to transient, distinct populations of Reptin as the monomer begins to assemble in the presence of ligand. When analyzing the HDX-MS data, we observed bimodal distributions of several wild-type Reptin peptides in samples with ATP that were not present in the Reptin^{Y340A} mutant. An illustration of bimodal spectra is in Fig. 7. These peptides were located in the ATP pocket, specifically around the walker A motif in domain I and around the Y340 peptide docking motif in domain III. Notably, the bimodal isotopic envelops occurred only in peptides that exhibited conformational changes upon ligand binding. The Reptin-Pontin complex also exhibited bimodal distributions in the presence of ligand (Fig. 7). A bimodal distribution could result from EX1 HDX kinetics in which the rate of conformational change of the corresponding peptide is slower than the HDX rate. The other possible explanation of bimodal distribution is the presence of two different protein isoforms, and here it may arise from the distribution of monomeric and oligomeric forms of Reptin. This is supported by the fact that no bimodal distribution was detected in Reptin^{Y340A} (data not shown) and further, that the change in the pattern of deuteration appeared after the binding of ATP, which is known to initiate Reptin oligomerization. Moreover, the location of peptides with bimodal isotopic patterns also supports this interpretation, because the ATP pocket is located in between two Reptin molecules in the Reptin oligomer.

A complication of these data interpretation is that HDX-MS provides only an average of the deuteration of a given peptide length and does not necessarily provide fine-resolution mapping of a protein-protein interface. For example, our prior study discussed, using AGR2 as a model protein [36], that higher levels of deuterium suppression in a small stretch of the polypeptide are compensated by elevated deuteration in adjacent regions (due to conformational changes) so that the net deuteration in larger peptides is different than the smaller peptide. Thus, it is possible that this methodological limitation impacts on the number of deuterons measured in a given peptic fragment (as in Fig. 5). This limitation did not preclude the identification of regions whose deuteration can be altered through mutation of Y340. In addition, oligomeric proteins present a different problem which might relate to bimodal distributions (Fig. 7). When Reptin assembles into an oligomer, we do not know which monomer a given peptide originates from within the hexamer. A solution to this might be isotopic labelling of a Reptin pool so that upon mixing with normal isotopic Reptin, inter-subunit interactions might be revealed in the mixed olgiomer.

3.6. Use of molecular dynamic (MD) simulations to measure Reptin oligomerization dynamics

We carried out MD simulations to probe the above interpretations (Fig. 4). It is evident that the Y340 sidechain remains embedded in the adjacent subunit (Fig. 8A and C; Fig. 9C), stabilized by a hydrogen bond with the sidechain of Thr333 and also by packing interactions with the sidechains of Arg330 and Arg336 (all 3 residues belonging to the neighboring chain); this is seen in the MD simulations of both wild-type Reptin and in the D299N Reptin mutant (Supplementary Movie 1 and Supplementary Movie 3). In contrast, in the Y340A Reptin mutant (Fig. 8B; Fig. 9D), the sidechain Ala has no polar groups to form the hydrogen bond, resulting in the loop containing Y340 moving away by about 5 Å. The buried surface areas between the monomers (Fig. 9A in the wild-type Reptin and the D299N mutant) remain similar in their liganded states while the *apo* form of wild-type Reptin samples two states – one that resembles the packed liganded states and the other more open state which is similar to that sampled by the Y340A mutant

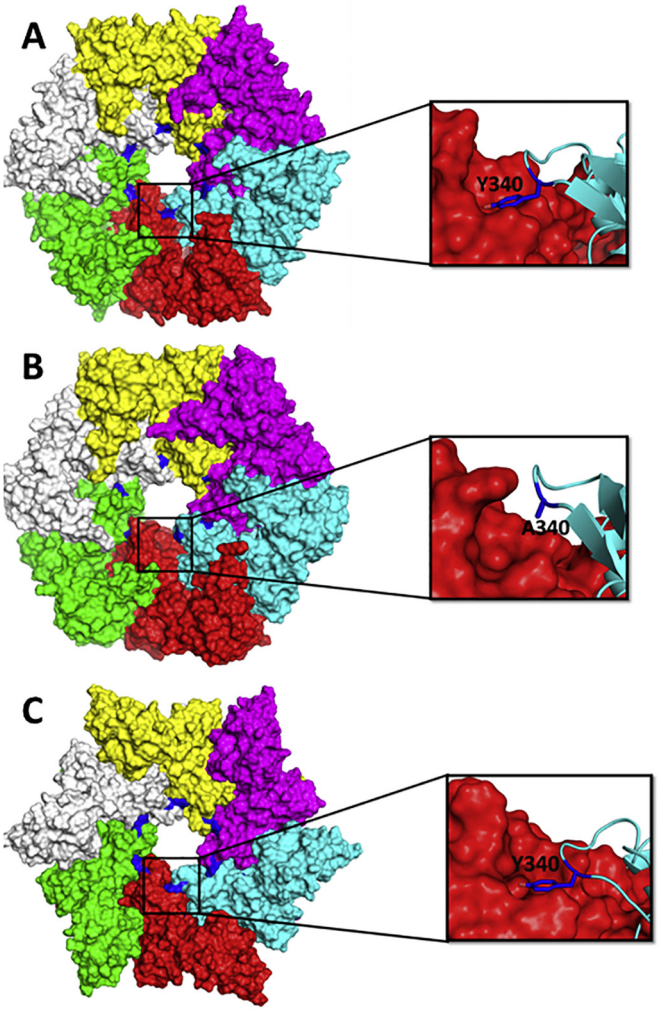

Fig. 8. MD simulation guided modeling of Reptin oligomerization. A snapshot is depicted from the MD simulations of (A). wild-type Reptin, (B). the Y340A mutant form of Reptin and (C). the D299N mutant form of Reptin, as hexamers. Although the Y340A mutant form of reptin may not exist as a hexamer, the structural changes during the MD simulations, which were initiated from the hexameric wild type structure, show that the mutation results in loss of key stabilizing interactions, which would likely result in the dissociation of the hexamer (this dissociation would require very long simulation times). Each monomer unit is colored differently with the Tyrosine finger (Y340) highlighted in blue colour. The data can be visualized in Supplementary movies 1-3. (For interpretation of the references to colour in this figure legend, the reader is referred to the web version of this article.)

which loses key interactions that stabilize the hexamer (Supplementary Movie 2).

As a control, D299N Reptin is very stable because the interface near the sidechain of D299 is anionic with several negatively charged groups (arising from the sidechains of E107, E300 and the phosphate of the ligand in the same chain as D299 and the sidechains of D349 and D352 from the neighboring chain, all within 8–9 Å of D299). The loss of the anionic sidechain of D299 in the D299N mutation results in the attenuation of the repulsions; in addition, the N299 sidechain is further stabilized by a water mediated interaction with D349 from the neighboring chain (Fig. 9A and B). This is also apparent in snapshots from the MD simulations (Supplementary Movies 1-3).

4. Discussion

Reptin forms a model AAA+ superfamily member with which to develop new approaches for dissecting stages in ligand-mediated oligomer assembly. In the past thirty years, the dominant tools used by proteomics approaches to discovery protein-interactions have been; (i) the yeast two hybrid; and (ii) immuno-precipitations. It is also now known that the vast diversity of protein interaction dynamics in higher eukaryotes appear to be regulated by small linear peptide motifs (27). Linear motifs in peptides can form 'hotspots' that play dominant role in driving protein-protein interactions and might form key target for drugging protein-protein interactions [38,39]. A classic example is the oncogenic protein MDM2; which can form a high affinity interaction with a small synthetic peptide derived from the p53 tumor suppressor [40] and which has been the basis for drug that target the linear peptide binding pocket of MDM2 [41].

Thus, a methodological approach for identifying hotspot protein-peptide interaction sites is using either synthetic peptides or phage-combinatorial peptide libraries [42]. Overlapping synthetic peptide scan assays using peptides derived from the open reading frame of Reptin were used to determine whether self-peptides that interact stably with Reptin itself, could be identified. This approach revealed a relatively high affinity, self-assembly interface that stabilizes the Reptin hexamer (dominating by Tyrosine 340). Only one self-binding motif for Reptin was identified (peptide 28; Fig. 1). For example, peptides derived from the an inter-subunit interface region of Reptin (amino acids ~420–440) did not bind Reptin in this assay. This highlights a limitation of this assay; it can not necessarily identify any protein-protein contact dominated by linear peptide motifs. However, peptides that do bind in such assays form compelling models to dissect out mechanisms of linear-peptide-protein docking.

The single dominating self-peptide maps to the Reptin hexameric "rim" (Fig. 1B), with a Tyrosine residue (Y340) forming an inter-subunit stabilizing anchor (Figs. 8-9). The subunit that interacts with the tyrosine-containing donor peptide forms a small acceptor pocket (Fig. 9). Size exclusion chromatography affirmed that ligand-induced oligomerization of mutant Y340A Reptin is attenuated (Fig. 3B).

There is presumably combinatorial diversity in this Y340 donor-acceptor docking reaction. Although the Y340 side chain forms an important stabilizing contact in a Reptin-Reptin homo-oligomer, it might not be as important in a Reptin-Pontin hetero-oligomer (Fig. 6C). Further, whether the 'rim' of a Pontin-Pontin oligomer also forms a hotspot stabilizing contact in this vicinity requires additional functional studies. An unexpected result from our studies, that complements the identification of Y340 as an important driver of Reptin assembly, was the impact of the D299N mutation on oligomerization.

The D299N version of Reptin, lacks ATPase activity and has classically been used as a 'loss-of-function' mutant [33]. However, this mutant has an elevated ATP-binding activity [13]. In our current study, we can interpret the data that the D299N mutant produces a spontaneous oligomer in the absence of ligand (Fig. 3C). Molecular Dynamics simulations show that the ability of Y340A Reptin to form stable oligomers is attenuated because of the loss of the hydrogen bond and packing afforded by the sidechain of Y340 against neighboring monomers (Fig. 8-9). However, in the D299N Reptin mutant, destabilizing, negatively charged inter-subunit contacts are removed, resulting in the stabilization of the hexamer in the absence of ligand (Fig. 9; Movie 3). This gives a more complex interpretation to cell based studies using the D299N mutant of Reptin. Its inhibitory effect on growth could be because of (i) defects in ATPase function; (ii) elevated ATP-binding; or (iii) elevated spontaneous oligomerization (this study). In the latter case, since Reptin's specific activity in protein-binding assays is regulated by its monomer and oligomerization status (Fig. 4), then in cells the Reptin^{D299N} mutant could be inhibitory for cell growth because of alterations in its interactome.

In conclusion, our pipeline approach for dissecting 'hotspot' interactions in one AAA+ family member provides a blueprint to produce functional mutants based on self-assembly peptide motif scans. Our data highlight a novel linear motif in Reptin that forms an inter-subunit

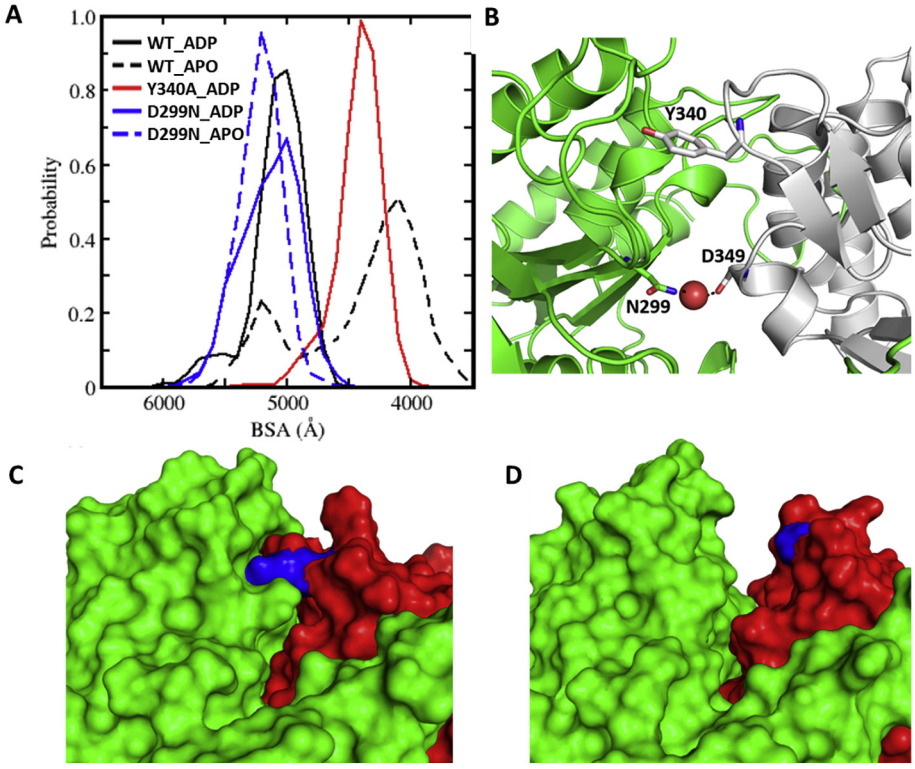

Fig. 9. Evaluation of the D299N and Y340A forms of Reptin. (A). Distribution of buried surface area (BSA) of the inter-subunit protein-protein interface calculated from the conformations sampled during the MD simulations of wildtype and mutant Reptin hexamers in their *apo* and ADP bound states. The BSA was calculated by subtracting the solvent accessible surface area (SASA) of the inter-subunit protein-protein interface from the sum of the SASA of each monomer. (B). MD snapshot of the Reptin hexamer showing water mediated interactions between two monomers. Residues (N299 from monomer A and D349 from monomer B) involved in water mediated interactions are highlighted in sticks, the water molecule is shown as a red sphere and water-mediated hydrogen bond interactions are shown as dashed lines. (C). Snapshot from the MD simulations highlighting the tight packing between the two monomers (colored green and red) in the case of wild-type Reptin and (D). loss in packing interactions due to the Y340A mutation. Reptin is depicted as surface, and Y340 and A340 are highlighted in blue colour. (For interpretation of the references to colour in this figure legend, the reader is referred to the web version of this article.)

bridge that appears to play a role in hexamer stability. Such mutant forms of Reptin (Y340A) can be used in the future in cell systems to dissect the interactome of Reptin as a function of monomer to oligomer states (Fig. 4). There is a precedent for the ability of small peptides to interact with dynamic forms of Reptin; a recent biochemical study evaluated the impact of histones on Reptin and Pontin transcriptional regulation [43]. The authors identified histone-3 peptides that not only regulate the monomer-oligomer transition of Reptin and Pontin but showed that endogenous proteins immuno precipitated by monomeric Reptin are distinct from proteins that interact with oligomers. These data highlight the functional importance of Reptin oligomerization in controlling its interactome (as in Fig. 4 and [43]).

Supplementary data to this article can be found online at https://doi.org/10.1016/j.jprot.2019.02.012.

Acknowledgements

The work was supported by: the Czech Science Foundation 16-20860S (PM, LH) and 16-07321S (BV, TH), the project MEYS – NPS I – LO1413, and MH CZ - DRO (MMCI, 00209805); the BBSRC RASOR consortium (BB/C511599/1; United Kingdom); Cancer Research UK (C21383/A6950); The International Centre for Cancer Vaccine Science project carried out within the International Research Agendas programme of the Foundation for Polish Science co-financed by the European Union under the European Regional Development Fund; A*STAR, Singapore and NSCC, Singapore.

References

[1] R.T. Sauer, D.N. Bolon, B.M. Burton, R.E. Burton, J.M. Flynn, R.A. Grant, G.L. Hersch, S.A. Joshi, J.A. Kenniston, I. Levchenko, S.B. Neher, E.S. Oakes, S.M. Siddiqui, D.A. Wah, T.A. Baker, Sculpting the proteome with AAA(+) proteases and disassembly machines, Cell 119 (1) (2004) 9–18.
[2] R.T. Sauer, T.A. Baker, AAA+ proteases: ATP-fueled machines of protein destruction, Annu. Rev. Biochem. 80 (2011) 587–612.
[3] P.M. Matias, S. Gorynia, P. Donner, M.A. Carrondo, Crystal structure of the human AAA+ protein RuvBL1, J. Biol. Chem. 281 (50) (2006) 38918–38929.
[4] S. Gorynia, T.M. Bandeiras, F.G. Pinho, C.E. McVey, C. Vonrhein, A. Round, D.I. Svergun, P. Donner, P.M. Matias, M.A. Carrondo, Structural and functional insights into a dodecameric molecular machine - the RuvBL1/RuvBL2 complex, J. Struct. Biol. 176 (3) (2011) 279–291.
[5] M. Petukhov, A. Dagkessamanskaja, M. Bommer, T. Barrett, I. Tsaneva, A. Yakimov, R. Queval, A. Shvetsov, M. Khodorkovskiy, E. Kas, M. Grigoriev, Large-scale conformational flexibility determines the properties of AAA+ TIP49 ATPases, Structure 20 (8) (2012) 1321–1331.
[6] J. Jin, Y. Cai, T. Yao, A.J. Gottschalk, L. Florens, S.K. Swanson, J.L. Gutierrez, M.K. Coleman, J.L. Workman, A. Mushegian, M.P. Washburn, R.C. Conaway, J.W. Conaway, A mammalian chromatin remodeling complex with similarities to the yeast INO80 complex, J. Biol. Chem. 280 (50) (2005) 41207–41212.
[7] T.L. Clarke, M.P. Sanchez-Bailon, K. Chiang, J.J. Reynolds, J. Herrero-Ruiz, T.M. Bandeiras, P.M. Matias, S.L. Maslen, J.M. Skehel, G.S. Stewart, C.C. Davies, PRMT5-Dependent Methylation of the TIP60 Coactivator RUVBL1 Is a Key Regulator of Homologous Recombination, Mol. Cell. 65 (5) (2017) 900–916 e7.
[8] L. Gnatovskiy, P. Mita, D.E. Levy, The human RVB complex is required for efficient transcription of type I interferon-stimulated genes, Mol. Cell. Biol. 33 (19) (2013) 3817–3825.
[9] S.G. Cho, A. Bhoumik, L. Broday, V. Ivanov, B. Rosenstein, Z. Ronai, TIP49b, a regulator of activating transcription factor 2 response to stress and DNA damage, Mol. Cell. Biol. 21 (24) (2001) 8398–8413.
[10] P. Bellosta, T. Hulf, S. Balla Diop, F. Usseglio, J. Pradel, D. Aragnol, P. Gallant, Myc interacts genetically with Tip48/Reptin and Tip49/Pontin to control growth and proliferation during Drosophila development, Proc. Natl. Acad. Sci. U. S. A. 102 (33) (2005) 11799–11804.
[11] S. Rashid, I. Pilecka, A. Torun, M. Olchowik, B. Bielinska, M. Miaczynska, Endosomal adaptor proteins APPL1 and APPL2 are novel activators of beta-catenin/TCF-mediated transcription, J. Biol. Chem. 284 (27) (2009) 18115–18128.
[12] C. Xie, W. Wang, F. Yang, M. Wu, Y. Mei, RUVBL2 is a novel repressor of ARF transcription, FEBS Lett. 586 (4) (2012) 435–441.
[13] M.M. Maslon, R. Hrstka, B. Vojtesek, T.R. Hupp, A divergent substrate-binding loop within the pro-oncogenic protein anterior gradient-2 forms a docking site for Reptin, J. Mol. Biol. 404 (3) (2010) 418–438.
[14] N. Izumi, A. Yamashita, A. Iwamatsu, R. Kurata, H. Nakamura, B. Saari, H. Hirano, P. Anderson, S. Ohno, AAA+ proteins RUVBL1 and RUVBL2 coordinate PIKK activity and function in nonsense-mediated mRNA decay, Sci. Signal. 3 (116) (2010) ra27.
[15] A.S. Venteicher, Z. Meng, P.J. Mason, T.D. Veenstra, S.E. Artandi, Identification of ATPases pontin and reptin as telomerase components essential for holoenzyme assembly, Cell 132 (6) (2008) 945–957.
[16] A. Rivera-Calzada, M. Pal, H. Munoz-Hernandez, J.R. Luque-Ortega, D. Gil-Carton, G. Degliesposti, J.M. Skehel, C. Prodromou, L.H. Pearl, O. Llorca, The Structure of the R2TP Complex Defines a Platform for Recruiting Diverse Client Proteins to the HSP90 Molecular Chaperone System, Structure 25 (7) (2017) 1145–1152 e4.
[17] J. Rosenbaum, S.H. Baek, A. Dutta, W.A. Houry, O. Huber, T.R. Hupp, P.M. Matias, The emergence of the conserved AAA+ ATPases Pontin and Reptin on the signaling landscape, Sci. Signal. 6 (266) (2013) mr1.

[18] A.R. Healy, D.R. Houston, L. Remnant, A.S. Huart, V. Brychtova, M.M. Maslon, O. Meers, P. Muller, A. Krejci, E.A. Blackburn, B. Vojtesek, L. Hernychova, M.D. Walkinshaw, N.J. Westwood, T.R. Hupp, Discovery of a novel ligand that modulates the protein-protein interactions of the AAA+ superfamily oncoprotein reptin, Chem. Sci. 6 (5) (2015) 3109–3116.
[19] J.K. Murray, S.H. Gellman, Targeting protein-protein interactions: lessons from p53/MDM2, Biopolymers 88 (5) (2007) 657–686.
[20] M. Durech, F. Trcka, P. Man, E.A. Blackburn, L. Hernychova, P. Dvorakova, D. Coufalova, D. Kavan, B. Vojtesek, P. Muller, Novel Entropically driven conformation-specific interactions with Tomm34 protein modulate Hsp70 protein folding and ATPase activities, Mol. Cell. Proteomics 15 (5) (2016) 1710–1727.
[21] D. Kavan, P. Man, MSTools—web based application for visualization and presentation of HXMS data, Int. J. Mass Spectrom. 302 (2011) 53–58.
[22] M. Guttman, D.D. Weis, J.R. Engen, K.K. Lee, Analysis of overlapped and noisy hydrogen/deuterium exchange mass spectra, J. Am. Soc. Mass Spectrom. 24 (12) (2013) 1906–1912.
[23] W.L. DeLano, PyMOL, 700 DeLano Scientific, San Carlos, CA, 2002.
[24] D.A. Case, V. Babin, J.T. Berryman, R.M. Betz, Q. Cai, D.S. Cerutti, T.E. Cheatham, T.A. Darden, R.E. Duke, H. Gohlke, A.W. Goetz, S. Gusarov, N. Homeyer, P. Janowski, J. Kaus, I. Kolossváry, A. Kovalenko, T.S. Lee, S. LeGrand, T. Luchko, R. Luo, B. Madej, K.M. Merz, F. Paesani, D.R. Roe, A. Roitberg, C. Sagui, R. Salomon-Ferrer, G. Seabra, C.L. Simmerling, W. Smith, J. Swails, J. Wang Walker, R.M. Wolf, X. Wu, P.A. Kollman, Amber14, University of California, San Francisco, 2014.
[25] J.A. Maier, C. Martinez, K. Kasavajhala, L. Wickstrom, K.E. Hauser, C. Simmerling, ff14SB: Improving the Accuracy of Protein Side Chain and Backbone Parameters from ff99SB, J. Chem. Theory Comput. 11 (8) (2015) 3696–3713.
[26] J. Wang, R.M. Wolf, J.W. Caldwell, P.A. Kollman, D.A. Case, Development and testing of a general amber force field, J. Comput. Chem. 25 (9) (2004) 1157–1174.
[27] W.L. Jorgensen, J. Chandrasekhar, J. Madura, R.W. Impey, M.L. Klein, Comparison of simple potential functions for simulating liquid water, J. Chem. Phys. 79 (1983) 926–935.
[28] T. Darden, D. York, L. Pedersen, Particle mesh Ewald: an Nlog (N) method for Ewald sums in large systems, J. Chem. Phys. 98 (1993) 10089–10092.
[29] S. Miyamoto, P.A. Kollman, Settle: an analytical version of the SHAKE and RATTLE algorithm for rigid water models, J. Comput. Chem. 13 (1992) 952–962.
[30] Y. Bromberg, G. Yachdav, Y. Ofran, R. Schneider, B. Rost, New in protein structure and function annotation: hotspots, single nucleotide polymorphisms and the 'Deep Web', Curr. Opin. Drug Discov. Devel. 12 (3) (2009) 408–419.
[31] P. Tompa, N.E. Davey, T.J. Gibson, M.M. Babu, A million peptide motifs for the molecular biologist, Mol. Cell 55 (2) (2014) 161–169.
[32] H. Benbahouche Nel, I. Iliopoulos, I. Torok, J. Marhold, J. Henri, A.V. Kajava, R. Farkas, T. Kempf, M. Schnolzer, P. Meyer, I. Kiss, E. Bertrand, B.M. Mechler, B. Pradet-Balade, Drosophila Spag is the homolog of RNA polymerase II-associated protein 3 (RPAP3) and recruits the heat shock proteins 70 and 90 (Hsp70 and Hsp90) during the assembly of cellular machineries, J. Biol. Chem. 289 (9) (2014) 6236–6247.
[33] A. Grigoletto, V. Neaud, N. Allain-Courtois, P. Lestienne, J. Rosenbaum, The ATPase activity of reptin is required for its effects on tumor cell growth and viability in hepatocellular carcinoma, Mol. Cancer Res. 11 (2) (2013) 133–139.
[34] L. Hernychova, P. Man, C. Verma, J. Nicholson, C.A. Sharma, E. Ruckova, J.Y. Teo, K. Ball, B. Vojtesek, T.R. Hupp, Identification of a second Nutlin-3 responsive interaction site in the N-terminal domain of MDM2 using hydrogen/deuterium exchange mass spectrometry, Proteomics 13 (16) (2013) 2512–2525.
[35] V. Narayan, V. Landre, J. Ning, L. Hernychova, P. Muller, C. Verma, M.D. Walkinshaw, E.A. Blackburn, K.L. Ball, Protein-protein interactions modulate the docking-dependent E3-ubiquitin ligase activity of Carboxy-terminus of Hsc70-interacting protein (CHIP), Mol. Cell. Proteomics 14 (11) (2015) 2973–2987.
[36] M.A. Mohtar, L. Hernychova, J.R. O'Neill, M.L. Lawrence, E. Murray, B. Vojtesek, T.R. Hupp, The sequence-specific peptide-binding activity of the protein Sulfide Isomerase AGR2 directs its stable binding to the oncogenic receptor EpCAM, Mol. Cell. Proteomics 17 (4) (2018) 737–763.
[37] F. Trcka, M. Durech, P. Man, L. Hernychova, P. Muller, B. Vojtesek, The assembly and intermolecular properties of the Hsp70-Tomm34-Hsp90 molecular chaperone complex, J. Biol. Chem. 289 (14) (2014) 9887–9901.
[38] H. Jubb, A.P. Higueruelo, A. Winter, T.L. Blundell, Structural biology and drug discovery for protein-protein interactions, Trends Pharmacol. Sci. 33 (5) (2012) 241–248.
[39] A. Ciulli, G. Williams, A.G. Smith, T.L. Blundell, C. Abell, Probing hot spots at protein-ligand binding sites: a fragment-based approach using biophysical methods, J. Med. Chem. 49 (16) (2006) 4992–5000.
[40] S.M. Picksley, B. Vojtesek, A. Sparks, D.P. Lane, Immunochemical analysis of the interaction of p53 with MDM2;–fine mapping of the MDM2 binding site on p53 using synthetic peptides, Oncogene 9 (9) (1994) 2523–2529.
[41] L.T. Vassilev, B.T. Vu, B. Graves, D. Carvajal, F. Podlaski, Z. Filipovic, N. Kong, U. Kammlott, C. Lukacs, C. Klein, N. Fotouhi, E.A. Liu, In vivo activation of the p53 pathway by small-molecule antagonists of MDM2, Science 303 (5659) (2004) 844–848.
[42] H. Shimizu, L.R. Burch, A.J. Smith, D. Dornan, M. Wallace, K.L. Ball, T.R. Hupp, The conformationally flexible S9-S10 linker region in the core domain of p53 contains a novel MDM2 binding site whose mutation increases ubiquitination of p53 in vivo, J. Biol. Chem. 277 (32) (2002) 28446–28458.
[43] R. Queval, C. Papin, M. Dalvai, K. Bystricky, O. Humbert, Reptin and Pontin oligomerization and activity are modulated through histone H3 N-terminal tail interaction, J. Biol. Chem. 289 (49) (2014) 33999–34012.